JOURNAL OF AGRICULTURAL AND FOOD CHEMISTRY

Article

pubs.acs.org/JAFC

Engineering Functional Nanothin Multilayers on Food Packaging: Ice-Nucleating Polyethylene Films

Zafer Gezgin,[‡] Tung-Ching Lee,[†] and Qingrong Huang*[,†]

[†]Department of Food Science, Rutgers University, 65 Dudley Road, New Brunswick, New Jersey 08901-8520, United States

[‡]TÜBİTAK, The Scientific and Technological Research Council of Turkey, Tunus Caddesi No. 80, 06100 Kavaklıdere/Ankara, Turkey

ABSTRACT: Polyethylene is the most prevalent plastic and is commonly used as a packaging material. Despite its common use, there are not many studies on imparting functionalities to those films which can make them more desirable for frozen food packaging. Here, commercial low-density polyethylene (LDPE) films were oxidized by UV-ozone (UVO) treatment to obtain a negatively charged hydrophilic surface to allow fabrication of functional multilayers. An increase in hydrophilicity was observed when films were exposed to UVO for 4 min and longer. Thin multilayers were formed by dipping the UVO-treated films into biopolymer solutions, and extracellular ice nucleators (ECINs) were immobilized onto the film surface to form a functional top layer. Polyelectrolyte adsorption was studied and confirmed on silicon wafers by measuring the water contact angles of the layers and investigating the surface morphology via atomic force microscopy. An up to 4−5 °C increase in ice nucleation temperatures and an up to 10 min decrease in freezing times were observed with high-purity deionized water samples frozen in ECIN-coated LDPE films. Films retained their ice nucleation activity up to 50 freeze−thaw cycles. Our results demonstrate the potential of using ECIN-coated polymer films for frozen food application.

KEYWORDS: *low-density polyethylene (LDPE), UV-ozone (UVO) treatment, atomic force microscopy (AFM), extracellular ice nucleators (ECINs), ice nucleation, freezing curves*

INTRODUCTION

Nanotechnology, often described as the industrial revolution of our time, is the number one emerging technology in food science. Nanofoods are becoming more and more common, with the increasing use of nanotechnological methods in cultivation, production, processing, or packaging of foods.[1] The nanoenabled food and beverage packaging market was worth $4.13 billion in 2008 and is forecasted to grow to $7.3 billion by 2014, where the intelligent packaging segment is estimated to grow to $2.47 billion.[2] Despite many promising applications of food nanotechnology, such as molecular food creation or nutritional improvement of food constituents, still being regarded as future goals, nanotechnology is already being used by the food packaging industry.[1] This study focuses on a food packaging application of nanotechnology.

Low-density polyethylene (LDPE) is a thermoplastic obtained from petroleum and is commonly used to produce plastic bags, containers, and bottles. Much of the global demand for LDPE (67%) comes from the market of carrying bags, sacks, and films, such as agricultural, multilayer, and shrink films.[3] Such films are frequently pretreated either to increase their wettability or to modify their surface chemistry, which allows the adhesion of paint and ink or formation of composites via lamination.[4] Ultraviolet-ozone (UVO) treatment, a photosensitized oxidation method utilizing short-wavelength UV radiation to excite and dissociate molecules, has been used previously in the surface modification of polyethylene films.[4−6] Hydrocarbons excited with UV radiation at 253.7 nm react with the atomic oxygen that was generated by the dissociation of ozone at the same wavelength, which forms by the dissociation of molecular oxygen by UV radiation at 184.9 nm.[7] As the excited groups react with atomic oxygen and form volatile compounds such as CO_2, the concentration of hydrophilic groups such as carboxyl and aldehyde also increases on the surface, which consequently imparts increased wettability and overall negative charge to the treated surface.

Some methods currently being used in nanotechnology were already known before nanoscale instrumentation allowed us to review them with these tools. Layer by layer (LbL) deposition is one of these techniques, which is a simple yet powerful way of engineering nanothin polymer layers, allowing control over the molecular architecture and composition of the surface to be fabricated.[8] The ability to modify and design the structure of multilayers at a molecular level makes the LbL deposition technique superior to traditional methods such as film-casting and physical-chemical methods.[9] Application of this method dates back to the multilayer experiments of Iler with charged colloids in 1966[10] and later was shown by Fromherz in 1980 with protein−polyelectrolyte multilayers.[11]

Recent applications of nanothin biopolymer multilayer deposition are more focused on designing devices for the biomedical industry that contain bioactive molecules; reports published in the past decade explore the control of the film inner structure and their mechanical properties by diffusing molecules into them or designing reservoirs to hold the target molecules.[12] LbL deposition of chitosan and hyaluronan was studied as an antimicrobial coating[13] and of chitosan and

Received: February 4, 2013
Revised: April 21, 2013
Accepted: April 23, 2013
Published: April 23, 2013

heparin as an antimicrobial and antiadhesive multilayer surface which can potentially be used for the surface modification of cardiovascular devices.[14] The poly(L-glutamic acid) and chitosan pair was used to create a bioactive multilayer coating which promotes muscle myoblast cell attachment and growth.[15] Alternatively, we experimented with another positively charged biopolymer, poly-ε-lysine, in this study to replace chitosan.

We used the LbL deposition technique to fabricate nanothin layers on LDPE substrates by dipping them in positively and negatively charged biopolymer solutions consecutively to build ultrathin multilayers that possess ice nucleation functionality due to the top extracellular ice nucleator (ECIN) layer. ECINs are biogenic ice nucleators, a term which is generally used to define substances which can trigger ice nucleation at −10 °C or higher.[16] A number of bacteria from the *Erwinia*, *Pseudomonas*, and *Xanthamonas* genuses produce this extracellular matter as an adaptation product to protect themselves from intracellular cell rupture that results from ice crystal growth at subzero temperatures by reducing ice crystal size through faster freezing.[17]

ECINs were mixed into foods and studied extensively to evaluate the improved freeze−thaw resistance[18] and energy-saving[19−27] potentials; however, application of ECINs as a nanothin layer has not been investigated. In this study, we fabricated multilayers on UVO-treated LDPE substrates using the LbL deposition technique through the electrostatic interaction of oppositely charged polyelectrolytes. We studied the ice nucleation activity of ECIN-coated LDPE films with high-purity deionized water by collecting their freezing curves on a cooling bath to explore the potential of using this functional packaging film on aqueous-based frozen foods.

MATERIALS AND METHODS

Materials. LDPE films were obtained by cutting and using the inner surface of sterile TWIRL'EM sampling bags (EFL-1012) manufactured by Labplas (Quebec, Canada), in accordance with FDA regulations. ECINs obtained from *Erwinia herbicola* ssp. *ananas* (catalog no. 11530, ATCC, Rockville, MD), a bacterium which was renamed to *Pantoea ananas* in 1995,[27] were used throughout the study. Cationic poly(diallyldimethylammonium chloride) (PDDA) and anionic poly(styrenesulfonate) (PSS), H_2O_2, H_2SO_4, and iota carrageenan (type II, CAS no. 9062-07-1) were purchased from Sigma-Aldrich (Milwaukee, WI), and all chemicals were used as received without further purification. Poly-ε-lysine (ε-PL) was purchased from Zhejiang Silver-Elephant Bioengineering Co., Ltd. (China). Silicon wafers were purchased from Montco Silicon Technologies (Spring City, PA). In all procedures, ultrapure water (Milli-Q plus system, Millipore) with a resistivity of 18.2 MΩ·cm was used.

Production and Isolation of Extracellular Ice Nucleators. ECINs were obtained and purified using the method described in ref 28. *E. herbicola* was grown at 18 °C in yeast extract for 24 h to the early stationary phase, followed by purification of ECINs using centrifugation, sonication, filtration, and ultracentrifugation. Then the pellet was suspended in 20 mM Tris buffer, freeze-dried, and stored at −20 °C.[23]

Film Preparation. As the first step, an LDPE bag was cut into 1 × 2 cm^2 pieces, and UV ozone treatment in the time range of 30 s to 10 min was applied using a UVO cleaner (model 42, Jelight Co. Inc., Irvine, CA), followed by water contact angle measurements.

A multilayer system of biopolymers was used to provide the positively charged surface for the adsorption of ECINs onto the LDPE film. ε-PL was used as the positively charged biopolymer where iota carrageenan (i-carr) was used as the negatively charged biopolymer. i-carr solution was prepared in 0.01 M NaCl and 0.01 M acetate buffer of pH 3.55. It was heated at 80 °C and stirred at this temperature using an impeller for 1 h and diluted 10-fold to obtain a concentration of 1 mg/mL. ECIN at 0.1 and 0.5 mg/mL and ε-PL at 1 mg/mL were prepared by stirring in Milli-Q water until they were fully dissolved. Solutions were filtered through 0.45 μm sized syringe filters (catalog no. 28143-286, VWR International, West Chester, PA).

Multilayers were prepared by initially dipping the UVO-treated LDPE film into the positively charged polymer, ε-PL, for 1 h followed by rinsing with Milli-Q water to get rid of the excess solution and drying it with a blow drier. Then the film was dipped into the i-carr solution for 20 min, followed by the same postprocedure, and then the procedure was repeated to build the third layer with ε-PL. The final layer was formed by dipping the film into the negatively charged ECIN solution for another 20 min, yielding a two-bilayer system on the polyethylene substrate.

For the initial experiment, coated and control LDPE films were folded and heat sealed from two sides using an impulse sealer (model AIE-300, American International Electric, Whittier, CA), then filled with Milli-Q water, and sealed from the top as the last step. The same procedure was followed with the untreated control. Afterward, both samples were cooled in a water/ethylene glycol bath to −6 °C.

Multilayer films were also deposited onto silicon wafers since the polyethylene film is too rough a substrate to image the polymers with atomic force microscopy (AFM). Wafers were cleaned earlier in a slightly boiled piranha solution (7:3 mixture of 98% H_2SO_4 and 30% H_2O_2) for 30 min, then rinsed with copious amount of Milli-Q water, and flushed with the nitrogen gas. The cleaned silicon wafers cut into 1 × 1 cm^2 pieces were immersed consecutively into the polyelectrolyte solutions to build the multilayers, as described above for the polyethylene substrate. The wafers were cleaned with Milli-Q water and flushed with gaseous nitrogen each time before being dipped in successive solutions. Wafers to be analyzed for surface morphology were placed in a Petri dish covered with punched Parafilm (Parafilm "M", Pechiney Plastic Packaging, Chicago, IL) to allow removal of moisture and vacuum-dried overnight prior to AFM measurement in an Isotemp vacuum oven (model 282-A, Fisher Scientific, Waltham, MA). On the following day, the top ECIN, ε-PL, and iota carragenan surfaces were imaged with AFM, and water contact angles were measured to determine hydrophilicity.

Verification of Ice Nucleation Activity. The activity of ECIN as an ultrathin layer was confirmed with a refrigerated water/ethylene glycol bath (model 1156D, VWR International, West Chester, PA), which was used to float the LDPE bags filled with Milli-Q water and to dip the vials in, which are coated on the inside with the LDPE films. For the experiments with the LDPE bags, the temperature was set to −6 °C and then reduced to −8 °C.

Freezing Curves. The inner walls (not the base) of a cylindrical minivial with a base diameter of 2 cm and a height of 4.5 cm were covered with an ECIN-coated LDPE film of ε-PL/i-carr/ε-PL/ECIN multilayers. The vial was refilled with 5 mL of fresh Milli-Q water before each freeze−thaw cycle, and 5 refills were done each day for 10 consecutive days, giving a total of 50 freeze−thaw cycles/freezing curves. Another vial which had an untreated film inside was used as a control and tested once each day, just like the ECIN-coated vial. To have a fixed cooling rate, the bath was adjusted to a fixed temperature of −15 °C for the testing of ECIN-coated films and controls. Setting the temperature to this level made certain that ice nucleation would occur in controls that do not possess ECINs. The temperature was fixed at −10 °C for the dipping solution concentration effect experiments. All other parameters such as the container type, sample volume, and dipping level were carefully checked in each step so that the cooling rate did not vary among trials. The inner temperature change was logged vs time every 2 s using an Omega OM-CP-TC-4000 datalogger system (Omega Engineering Inc., Stamford, CT).

Atomic Force Microscopy. Surface morphology was investigated with a Multimode Nanoscope IIIA atomic force microscope (Digital Instruments, Veeco Metrology, Santa Barbara, CA) which is operated in tapping mode. A silicon tip with an average drive frequency of 314 kHz was used for all images. Images of the layers of interest (1 × 1, 2 × 2, and 5 × 5 $μm^2$) were collected, and root-mean-square roughness

values were obtained as explained in further detail in the section "Statistical Analysis". All AFM experiments were carried out in air.

Water contact angles were measured using a VCA Optima video contact angle system (Advance SurfaceTechnology, Billerica, MA) to determine the changes in the wettability of polyethylene films as a function of the UV-ozone exposure time. It was also used to verify the adsorption and compare the hydrophilicity of the top biopolymer layers which were imaged with AFM. One condition to be able to use this very practical method to confirm surface modification is that the alternating polymers being used to build the multilayers have different wettabilities, so that the water contact angles of the more hydrophobic top layers will be higher than those of the more hydrophilic ones. Higher water contact angles indicate higher hydrophobicity, as the droplet tends to get flatter on the hydrophilic surfaces.

Quartz crystal microbalance with dissipation (QCM-D), a piezoelectric biosensor which can detect mass changes per unit area with an extremely high sensitivity of 0.4 ng/cm^2, was used to estimate the thickness of the layers formed during the LbL deposition process. A QCM-D apparatus (Q-Sense AB, Sweden) with a Q-Sense D300 electronic unit was used to detect the frequency changes. Plots of frequency shift versus time were obtained using the built-in Q-Sense software QSoft401. The data were used to estimate the layer thickness with the Kevin−Voigt model, assuming a fluid density of 1000 kg/m^3, a layer density of 1200 kg/m^3, and a dynamic viscosity of 0.001 kg/ms, as proposed for dilute biopolymer solutions in ref 29.

Statistical Analysis. Water contact angles of UVO-treated LDPE films and top biopolymer layers on silicon wafers were calculated by measuring the contact angles of at least 15 droplets. The standard deviations and means were automatically calculated from these values by the VCA Optima SPC statistical analysis software (Advance SurfaceTechnology, Billerica, MA). The freezing curve experiment was carried out in duplicate for the ECIN concentration effect. The mean ice nucleation temperature and time for an untreated film were calculated by averaging the data obtained from the 10 replicates, each collected after every 5 freeze−thaw cycles. AFM images were collected from at least five different regions on the wafer to confirm that the surface is uniform, and most representative images were used. Root-mean-square (rms) roughness (R_q) values were measured by the roughness analysis tool of the NanoScope Software 6.13 (Digital Instruments, Veeco Metrology, Santa Barbara, CA). The means and standard deviations were calculated from a minimum of 5 measurements obtained from several regions of the 1 × 1, 2 × 2, and 5 × 5 μm^2 images of each surface.

RESULTS AND DISCUSSION

Surface Modification of LDPE Films via UV-Ozone Treatment. Water contact angles of the UV-ozone-treated LDPE films decreased with increasing exposure times, yielding a more hydrophilic surface (Figure 1). There was a significant decrease in the average of advancing and receding water contact angles from above 75° to below 45° with longer than 3 min of UV-ozone exposure. The increase in wettability was in accordance with the earlier experiment of Zander et al.,[30] where contact angles decreased by approximately 35° following 5 min of UV-ozone treatment. The results also correlated well with the earlier observations of Mathieson et al.,[4] where the contact angles of polyethylene decreased by 30−40° and came to an equilibrium at around 3−5 min of exposure to UV-ozone. Similar results were observed with poly(ether ether ketone)[4,31] and polypropylene[32] as well.

The thicknesses of the four layers on a gold crystal as estimated by analyzing the QCM-D data with the Voigt model were 68 nm for the multilayers built using 0.1 mg/mL ECIN and 125 nm with 0.5 mg/mL ECIN (Figure 2). The thicknesses of the top ECIN layer alone were 17 and 100 nm for the multilayers formed with 0.1 and 0.5 mg/mL ECIN, respectively, which indicated the significant increase in layer thickness when

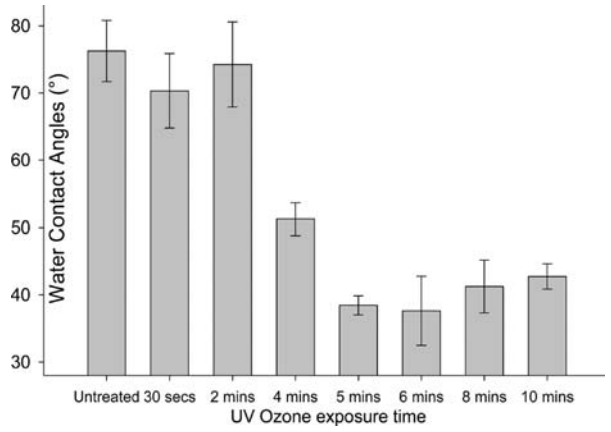

Figure 1. Variation of water contact angles with standard deviations of the LDPE film surface against the time of UV-ozone exposure.

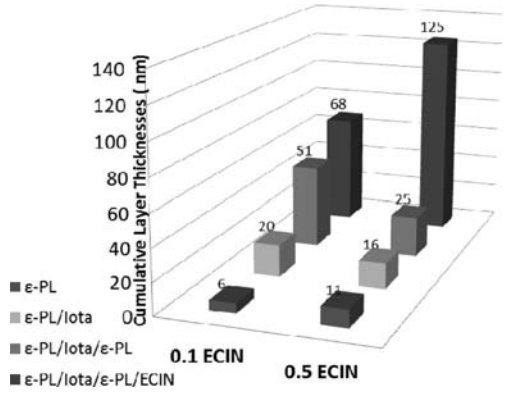

Figure 2. Cumulative layer thicknesses as predicted by the Voigt model for consecutive ε-PL/i-carr/ε-PL/ECIN layers where the top layer was formed by dipping into either 0.1 or 0.5 mg/mL ECIN solution.

the concentration of the ECIN dipping solution used to produce the top layer was increased. The thicknesses of the underlying i-carr and ε-PL layers were built by dipping the substrates into their 1 mg/mL solutions and varied in the range of 5−15 nm. The observation that the ECIN layers were thicker than pure polyelectrolyte layers is in accordance with the literature information regarding the composition of the extracellular ice-nucleating matter. ECINs have been proposed to be large molecules generally existing as lipoglycoproteins,[33] and there is a positive correlation between the aggregate size and ice nucleation activity.[17] The nucleant mass required to initiate ice nucleation at −2 °C was estimated to be around 19 000 kDa by Govindarajan and Lindow,[34] where the ideal (theoretical) and experimental molecular masses of i-carr were 543 and 482 kDa, respectively,[35] and that of ε-PL was reported as only 4.7 kDa.[36]

AFM Imaging of the Nanothin Layers Formed via LbL Deposition. Figure 3 shows the 1 × 1, 2 × 2, and 5 × 5 μm^2 AFM images of each of the four layers fabricated. Except for the first ε-PL layer, threads which belong to i-carr were observed in all images since the coverage of monolayers was not good enough to completely wrap the underlying polymer layer; hence, interpenetration of the layers occurred. Globular features seen on the first ε-PL layer, which are easier to see in Figure 4 since the z-scale was reduced from 50 to 10 nm, become almost invisible as more layers are built (Figure 3). This is due to the

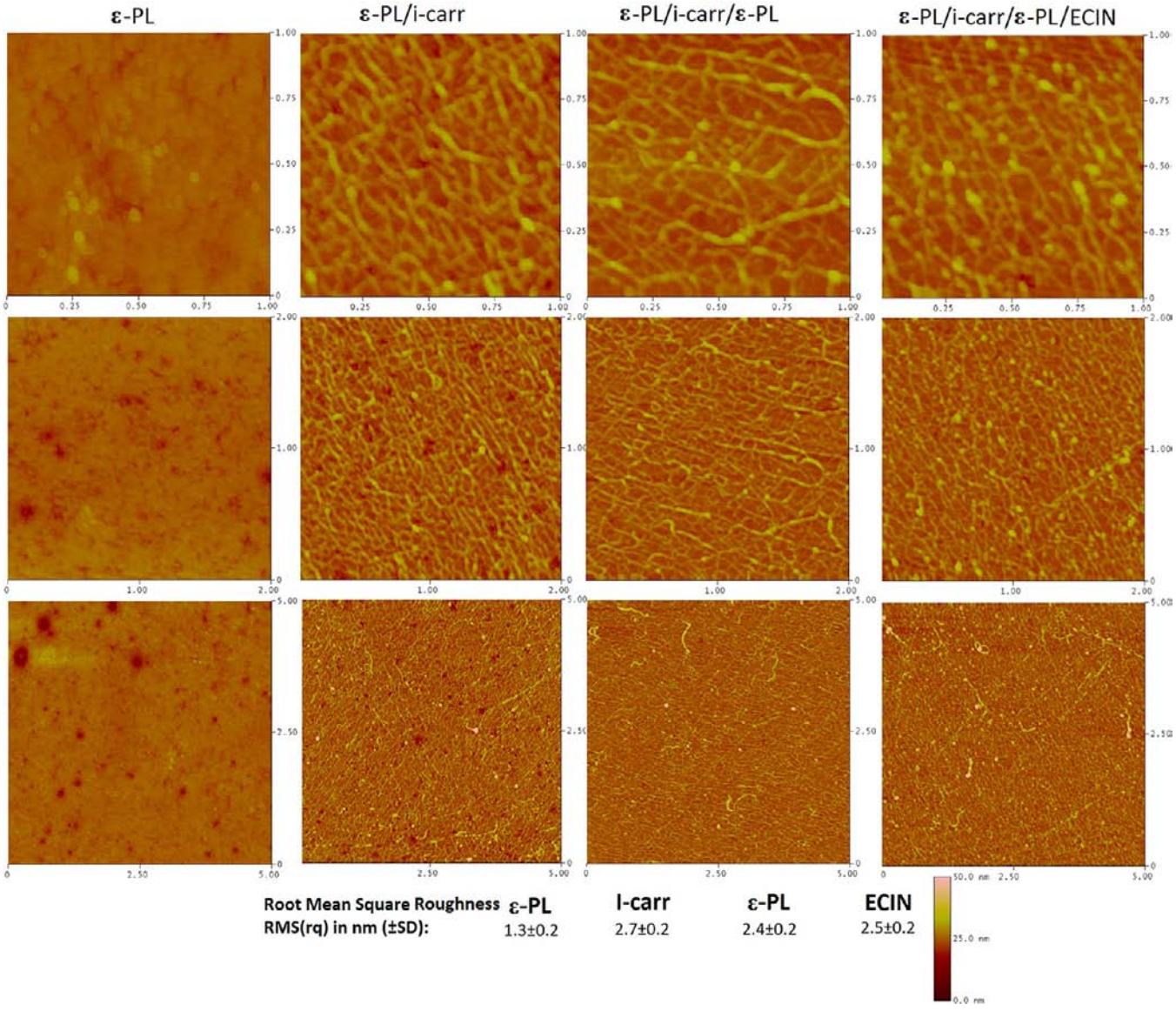

Figure 3. AFM images (1 ×1, 2 × 2, and 5 × 5 μm^2) and root-mean-square roughness ± standard deviation of the four nanothin layers (the *z*-scale is 50 nm).

shielding effect of the i-carr layer, threads of which were thicker than the globules of ε-PL. Thus, the roughness imparted by the i-carr threads made it impossible to distinguish ε-PL in those images unless they were located on those treads, mainly due to the attraction to the sulfate groups. Globules belonging to the ice nucleator proteins that come with the ECIN matter though were more visible and numerous on the fourth layer (Figure 3).

Ice Nucleation Activity of Nanothin ECIN Layers on Silicon Wafers. The silicon wafers used for AFM were placed on the cooling bath to concurrently analyze the ice nucleation activity on them. When the ice nucleation activity of the top ECIN, i-carr, and ε-PL layers was evaluated at −7 °C, only the droplets on the ECIN-coated wafers froze (Figure 5). Then the temperature was steadily decreased by 1 °C every 1/2 h, and the droplets on the i-carr and ε-PL top layers remained unfrozen until the temperature was dropped to −10 °C. This confirms that the ice nucleation observed at −7 °C is due to the presence of electrostatically absorbed ECIN matter on the surface and is not a random effect. This also verifies that the globular features on the top layer belong to the ECIN matter and not the underlying ε-PL layer on which the ECIN layer was formed.

In comparison to the multilayer systems of chitosan and i-carr studied by our group previously, a more organized gel network of i-carr was observed, with carrageenan threads almost lining parallel to each other (Figure 3). This provided a better foundation for layer buildup, allowing the even distribution of ε-PL and the negative charge on the surface. Thus, a more homogeneous layer of ECINs was fabricated, which increased the probability of simultaneous ice nucleation at multiple locations on the surface.

Wettability and Roughness of Nanothin Multilayers. Water contact angles measured indicated that the iota carrageenan layer was more hydrophilic than both the ECIN and ε-PL top layers (Figure 6). The wettabilities of the ECIN and ε-PL surfaces were similar. A correlation existed between hydrophilicity and root-mean-square roughness (rms/R_q), since the roughnesses of the ECIN and ε-PL layers were not significantly different and were lower than that of the i-carr surface (Figure 3). The roughness of a single layer of ε-PL on a

dx.doi.org/10.1021/jf400541q | J. Agric. Food Chem. 2013, 61, 5130−5138

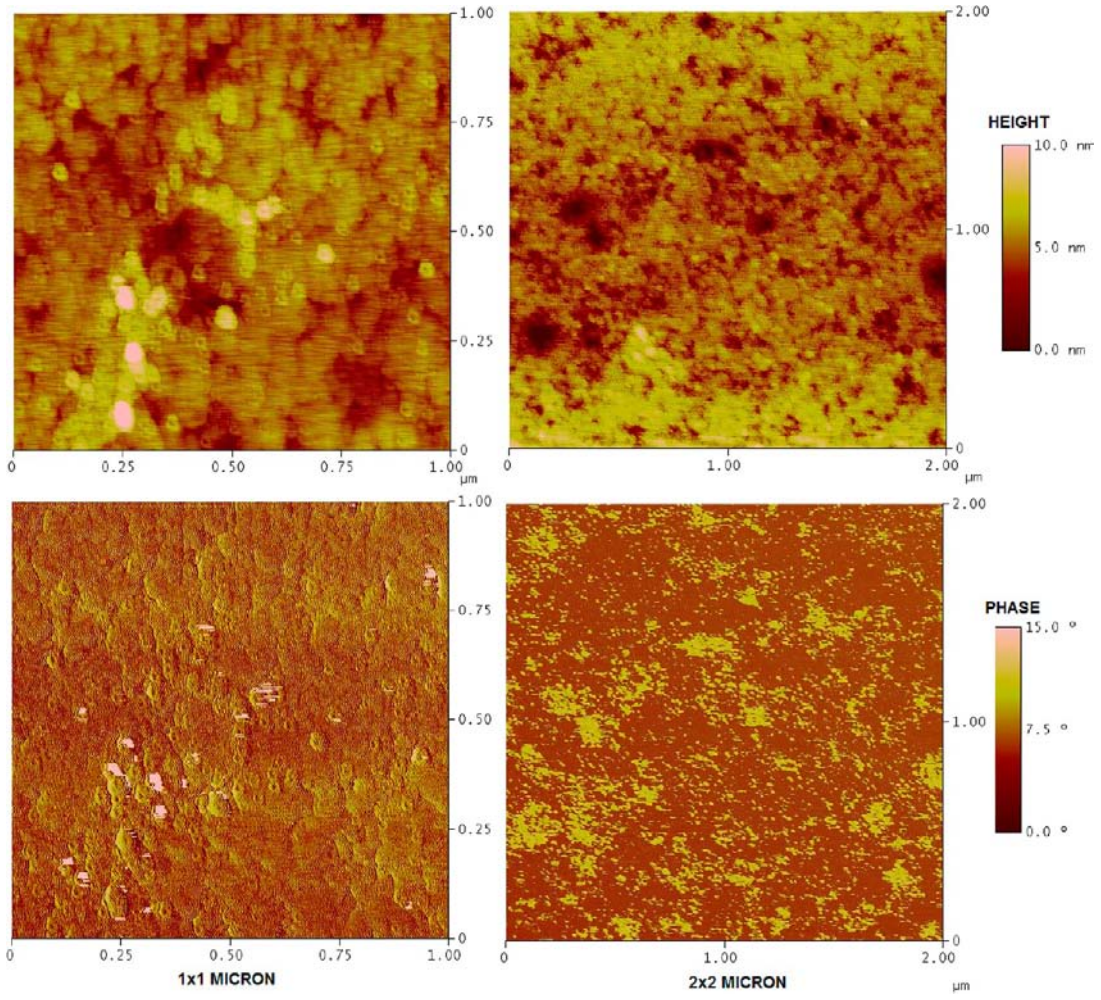

Figure 4. AFM height and phase images (1 ×1 and 2 × 2 μm^2) of a single layer of ε-PL on a silicon wafer (the z-scale is 10 nm).

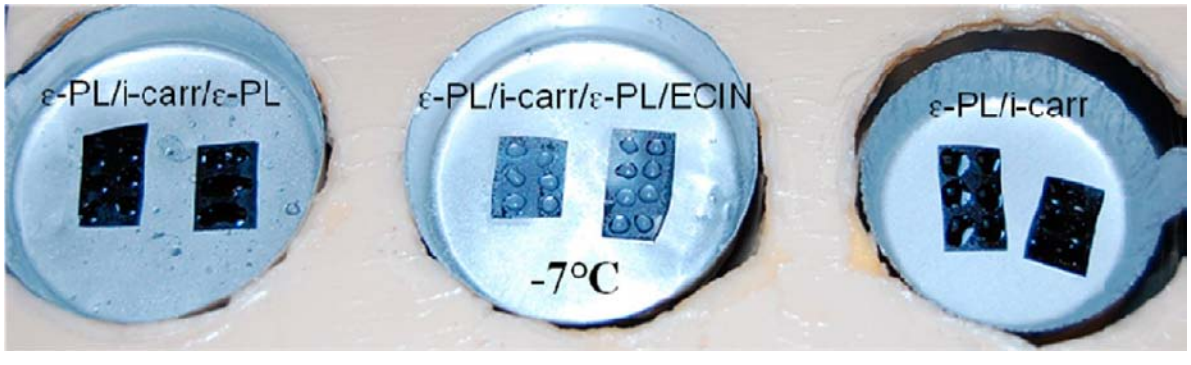

Figure 5. Freezing of 10 μL of high-purity dionized water droplets on ECIN, i-carr, and ε-PL top layers at −7 °C.

silicon wafer was 1.3 ± 0.2 nm. A significant increase in roughness from the second to fourth layer indicates the contribution of the carrageenan threads to the overall roughness of the surface.

Ice Nucleation Activity of Nanothin ECIN Layers on LDPE Films. After studying the nanoscale properties of this multilayer system and confirming the ice-nucleating activity on a silicon wafer, we fabricated these multilayers on a UVO-treated LDPE film substrate. When two bags of the same size, one made of ECIN-coated LDPE and the other made of untreated LDPE, and filled with identical amounts of Milli-Q water were cooled to −6 °C, ice nucleation occurred in the ECIN-coated film within 10 s, whereas the control stayed unfrozen for over 1 h (Figure 7). It should be noted that the ice nucleation temperature was higher than that when the nanothin ECIN layer was tested on a silicon wafer with 10 μL water droplets. This shows that when the sample volume increases, the probability of ice nucleation for the whole mass also increases. Although the amount of ECIN per unit area of the film did not change (also an important factor that increased the ice nucleation temperature and shortened the supercooling time, as observed in Figure 10), the contact area of water with the ECIN-coated surface increased when the volume became larger, and once an ice crystal has formed at one ice nucleation

dx.doi.org/10.1021/jf400541q | J. Agric. Food Chem. 2013, 61, 5130−5138

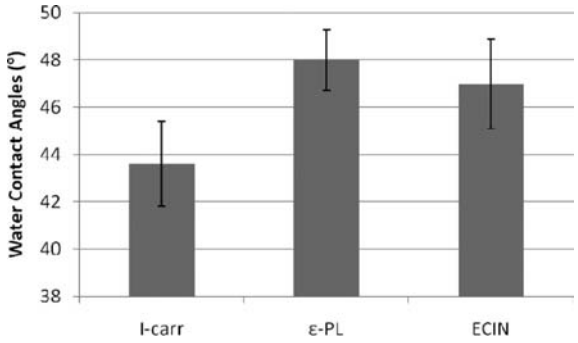

Figure 6. Water contact angles ± standard deviations of the top ECIN, i-carr, and ε-PL (third layer) layers.

Figure 7. Images of LDPE packaging materials filled with Milli-Q water and exposed to −6 °C, one without any treatment (left) and the other UV-ozone-treated on the inner surface followed by LbL deposition to form ε-PL/i-carr/ε-PL/ECIN multilayers (right).

site, it spreads quickly to the whole mass due to the high mobility of water molecules.

Reusability of ECIN-Coated LDPE Films. The reusability of the ice-nucleating film was investigated to evaluate the stability of the fabricated nanothin ECIN layer and see how long it took for the film to lose the initial activity. A stable film needing less frequent replacement could be used in a continuously running system to aid flash freezing, such as ice making. Reusability would also improve the freeze−thaw stability of foods meant to remain with the package through refrigeration, especially if those films were used in areas of the world where the cold chain was more susceptible to breakage. A total of 50 freeze−thaw cycles were conducted, where the Milli-Q water in the vial was thawed and the container refilled after each freezing curve was collected. The cooling rate and water volumes were fixed throughout the experiment. Figure 8 shows the freezing curves for the vial coated with the untreated control film and the 1st, 11th, 21st, 31st, 41st, and 50th refills for the vial coated with the ECIN-coated film. The average ice nucleation temperature in the control vial was −9.26 °C (the one shown in the graph with −9.68 °C was the final replicate). Ice nucleation temperatures in the vial laminated with the ECIN-coated LDPE varied in the range of −3.46 °C (on the 3rd refill) to −9.76 °C (on the 50th refill), with an average of −7.52 °C (Figure 9).

The average of the 1st plus 4 refills was 5.7 °C, and it stayed in the range of 7.01−7.93 °C until the 40th refill and then increased to 8.78 and 9.26 °C for the 45th and 50th refills, respectively, indicating a loss of activity over reuse. The experiment was discontinued at this point since the ice nucleation temperatures of the control and ECIN-coated film were proximate. For the first 45 freeze−thaw cycles, ice nucleation temperatures for the ECIN-coated vial were always

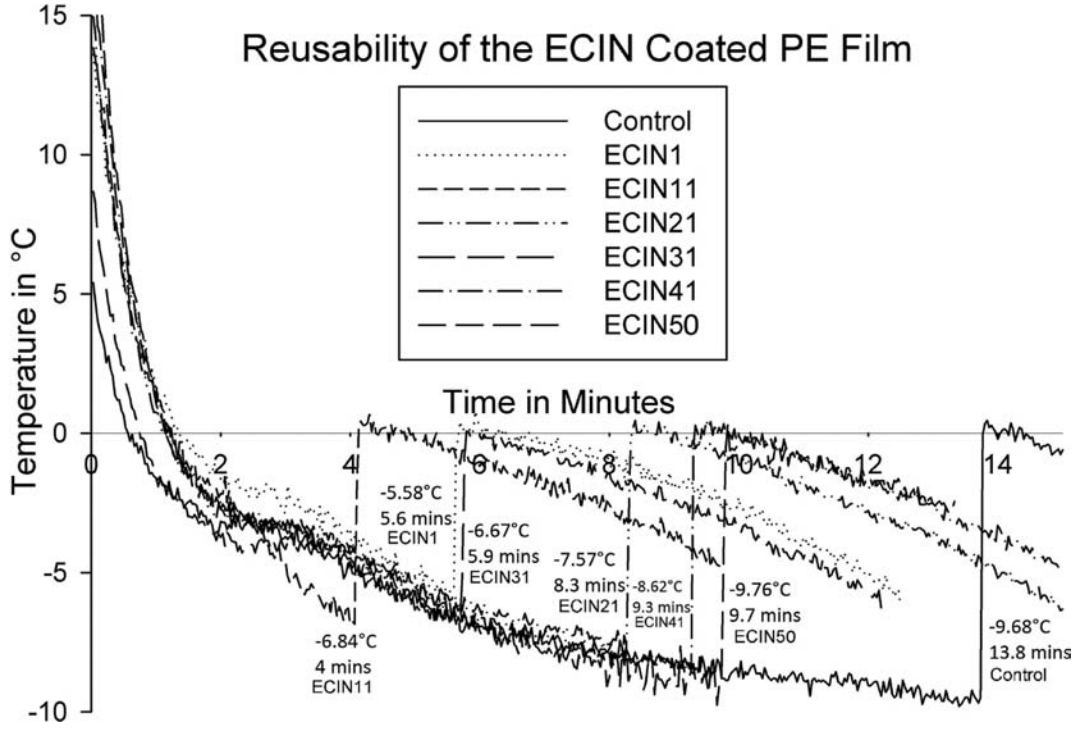

Figure 8. Freezing curves of 5 mL of pure water in minivials coated with the LDPE/ε-PL/i-carr/ε-PL/ECIN multilayer system and with untreated LDPE, up to 50 freeze−thaw cycles.

dx.doi.org/10.1021/jf400541q | J. Agric. Food Chem. 2013, 61, 5130−5138

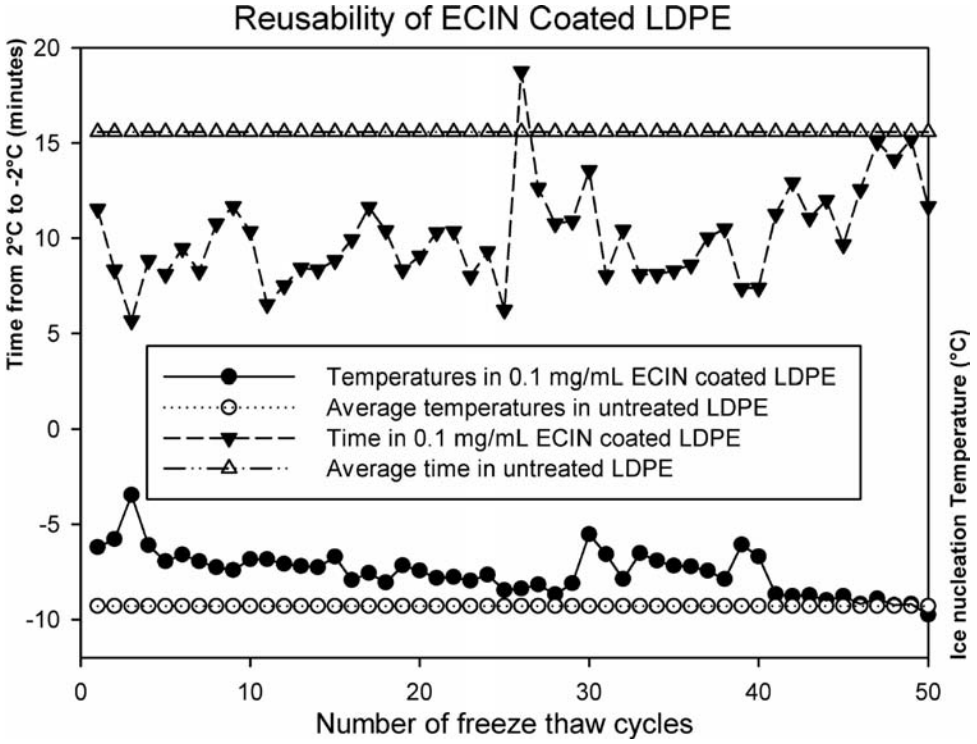

Figure 9. Variation in the ice nucleation temperatures and times (minutes from +2 to −2 °C) of 5 mL of pure water in minivials coated with the LDPE/ε-PL/i-carr/ε-PL/ECIN multilayer system versus the averages with the untreated LDPE, up to 50 freeze−thaw cycles.

higher than −9 °C, also higher than −8 °C during the first 17 refills and higher than −7 °C during the first 7 refills.

The time for the water to reach −2 °C from +2 °C at its geometric center, averaged from the 10 freezing curves of the control vial collected daily, was 15.6 min, where the shortest time for the water in ECIN-coated LDPE was 5.66 min, and the average time from 50 freezing curves was 10.10 min (Figure 9). A trend toward increasing ice nucleation times (the time point where freezing starts) with increased number of freeze−thaw cycles (refills) was observed. A correlation between the ice nucleation time and total freezing time (time it takes for the whole mass to reach the freezer temperature) also exists, which is indicated by the representative freezing curves in Figure 8 as well. This suggests that solely by increasing the ice nucleation temperature, which shortens the ice nucleation time, it is possible to save energy by decreasing the total freezing time. Additionally, since the sample volume of 5 mL is relatively small for the high cooling rate of our system, a phase change occurred almost instantaneously and the temperature continued to decline linearly to the water bath temperature. Thus, these experimental freezing curves look different from typical/theoretical freezing curves where an extended phase change stage can be seen as a straight line at the equilibrium freezing temperature until the whole mass turns into ice.

Effect of the Dipping Solution Concentration Used To Make the Nanothin ECIN Layer on the Freezing Curves of Pure Water. Figure 10 shows the freezing curves of LDPE films prepared by using 0.1 mg/mL (the same concentration was used for the reusability experiment) and 0.5 mg/mL ECIN solutions to make the top layer. Shorter ice nucleation times were observed for the higher concentration film in both curves, which indicated the higher probability of nucleation when the surface had more ice nucleation sites per unit area. The ice nucleation temperature with the first freezing curve was 4.16 °C

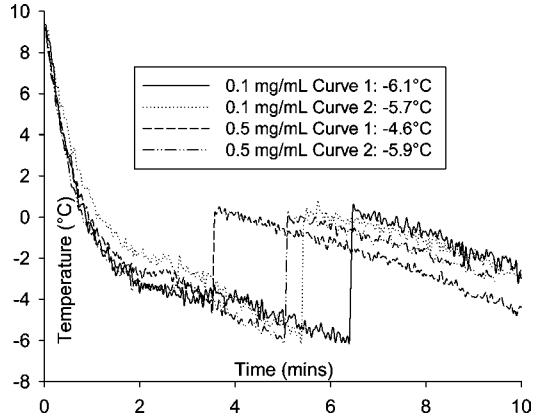

Figure 10. Freezing curves of 5 mL of pure water in minivials coated with the LDPE/ε-PL/i-carr/ε-PL/ECIN multilayer system, where ECIN dipping solution concentrations were 0.1 and 0.5 mg/mL.

for the 0.5 mg/mL film and 5.67 °C for the 0.1 mg/mL film (Figure 10).

Freezing Curves of the Dipping Solutions. Another test was conducted by filling the same vials with the dipping solutions instead with no film. Dramatically higher ice nucleation times were obtained with the 5 mL solutions of 0.1 and 0.5 mg/mL ECIN; all samples froze at temperatures higher than −1 °C and in less than 1.5 min (Figure 11). This shows that the activity of nanothin ECIN layers will be less than the activity observed when they are directly mixed into the samples to be frozen as studied extensively previously.[18−27] This is because the film cannot hold the large quantity of ECINs that the solution can, and with the films ice-nucleating sites are present only where the sample contacts the film, whereas in solution they are dispersed into the whole volume. Still, the use of nanothin films would be preferable where the

dx.doi.org/10.1021/jf400541q | J. Agric. Food Chem. 2013, 61, 5130−5138

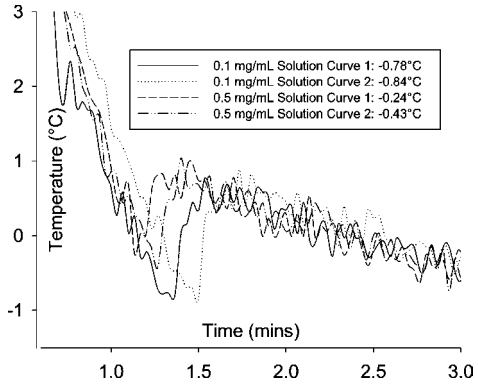

Figure 11. Freezing curves of 5 mL of ECIN solution at concentrations of 0.1 and 0.5 mg/mL.

ECINs cannot be added into the sample due to safety and/or sensory concerns.

In summary, novel ECIN-coated functional packaging films with higher freezing temperatures and shorter freezing times have been developed. Although formation of an ice nucleus is a very subtle phenomenon mostly expressed as a probability rate due to highly unpredictable behavior of water molecules making it hard to replicate freezing curves, in this study repeated tests clearly indicated a difference between the freezing of water in ECIN-coated films and that in nontreated films. The amount of energy remains constant from a thermodynamic point of view, but from a process standpoint, the achieved reduction in total freezing time means less energy consumption and thus lower costs for a constantly running freezing system.

This trial is a proof of concept for the possible application of cell-free ECIN-coated films as a functional packaging material to shorten the supercooling stage when freezing water and reduce the amount of energy required for this purpose. It also suggests the possible use of this approach to produce films of other functionalities (such as antimicrobial activity, etc.) via the LbL deposition technique, which is simple yet versatile. Future studies will be conducted with 20% sucrose solution and milk to see if the shortened freezing time effect with water can be reproduced with these samples. The effect of ECIN-coated LDPE films on the freeze−thaw stability of fish actomyosin will also be evaluated.

AUTHOR INFORMATION

Corresponding Author

*Phone: 848-932-5514. Fax: 732-932-6776. E-mail: qhuang@aesop.rutgers.edu.

Funding

This study was supported in part by USDA-NRI, Center of Advanced Food Technology (CAFT), and TÜBİTAK (The Scientific and Technological Research Council of Turkey).

Notes

The authors declare no competing financial interest.

REFERENCES

(1) Tiju, J.; Morrison, M. *Nanotechnology in Agriculture and Food*; Institute of Nanotechnology: Glasgow, Scotland, 2006.

(2) Plastemart. Bright future for nanotechnology in food & beverage packaging, 2010. http://www.plastemart.com/Plastic-Technical-Article.asp?LiteratureID=1379 (accessed Oct 17, 2010).

(3) Ceresana. Research market study: polyethylene LDPE, 2010. http://www.ceresana.com/en/market-studies/plastics/polyethylene-ldpe/polyethylene-ldpe-market-share-capacity-demand-supply-forecast-innovation-application-growth-production-size-industry.html (accessed June 15, 2010).

(4) Mathieson, I.; Bradley, R. H. Improved adhesion to polymers by UV/ozone surface oxidation. *Int. J. Adhes. Adhes.* **1996**, *16*, 29.

(5) Peeling, J.; Clark, D. T. Surface ozonation and photooxidation of polyethylene film. *J. Polym. Sci., Polym. Chem. Ed.* **1983**, *21*, 2047−2055.

(6) Ton-That, C.; Teare, D. O. H.; Campbell, P. A.; Bradley, R. H. Surface characterization of ultraviolet-ozone treated PET using atomic force microscopy and X-ray photoelectron spectroscopy. *Surf. Sci.* **1999**, *433*−*435*, 278.

(7) Ozcam, A. E.; Efimenko, K.; Jaye, C.; Spontak, R. J.; Fischer, D. A.; Genzer, J. Modification of PET surfaces with self-assembled monolayers of organosilane precursors. *J. Electron Spectrosc. Relat. Phenom.* **2009**, *172*, 95.

(8) Zhang, X.; Chen, H.; Zhang, H. Layer-by-layer assembly: from conventional to unconventional methods. *Chem. Commun.* **2007**, 1395−1405.

(9) Decher, G. Fuzzy nanoassemblies: toward layered polymeric multicomposites. *Science* **1997**, *277*, 1232−1237.

(10) Iler, R. K. Multilayers of colloidal particles. *J. Colloid Interface Sci.* **1966**, *21*, 569−594.

(11) Fromherz, P. *Assembling Proteins at Lipid Monolayers*; Springer Verlag: Berlin, 1980.

(12) Boudou, T.; Crouzier, T.; Ren, K.; Blin, G.; Picart, C. Multiple functionalities of polyelectrolyte multilayer films: new biomedical applications. *Adv. Mater.* **2009**, *21*, 1−27.

(13) Richert, L.; Lavalle, P.; Payan, E.; Shu, X. Z.; Prestwich, G. D.; Stoltz, J. F.; Schaaf, P.; Voegel, J. C.; Picart, C. Layer by layer buildup of polysaccharide films: physical chemistry and cellular adhesion aspects. *Langmuir* **2004**, *20*, 448−58.

(14) Fu, J.; Ji, J.; Yuan, W.; Shen, J. Construction of anti-adhesive and antibacterial multilayer films via layer-by-layer assembly of heparin and chitosan. *Biomaterials* **2005**, *26*, 6684−92.

(15) Song, Z.; Yin, J.; Luo, K.; Zheng, Y.; Yang, Y.; Li, Q.; Yan, S.; Chen, X. Layer-by-layer buildup of poly(L-glutamic acid)/chitosan film for biologically active coating. *Macromol. Biosci.* **2009**, *9*, 268−78.

(16) Lundheim, R. Physiological and ecological significance of biological ice nucleators. *Philos. Trans. R. Soc. London, B* **2002**, *357*, 937−943.

(17) Muryoi, N.; Kawahara, H.; Obata, H. Properties of a novel extracellular ice nuclei from ice-nucleating *Pseudomonas antarctica* IN-74. *Biosci., Biotechnol., Biochem.* **2003**, *67*, 1950−1958.

(18) Zhu, X.; Lee, T.-C. Application of a biogenic extra cellular ice nucleator for food processing: effects on the freeze-thaw stability of fish actomyosin from tilapia. *Int. J. Food Sci. Technol.* **2007**, *42*, 768−772.

(19) Hwang, W. Z.; Coetzer, C.; Tumer, N. E.; Lee, T. C. Expression of a bacterial ice nucleation gene in a yeast *Saccharomyces cerevisiae* and its possible application in food freezing processes. *J. Agric. Food Chem.* **2001**, *49*, 4662−6.

(20) Li, J.; Izquierdo, M. P.; Lee, T. C. Effects of ice-nucleation active bacteria on the freezing of some model food systems. *Int. J. Food Sci. Technol.* **1997**, *32*, 41.

(21) Li, J.; Lee, T.-C. Bacterial ice nucleation and its potential application in the food industry. *Trends Food Sci. Technol.* **1995**, *6*, 259.

(22) Li, J.; Lee, T.-C. Characterization of bacterial extracellular ice nucleators and their effects on the freezing of foods. Ph.D. Dissertation, Rutgers, State University of New Jersey, New Brunswick, 1998.

(23) Li, J.; Lee, T. C. Bacterial extracellular ice nucleator effects on freezing of foods. *J. Food Sci.* **1998**, *63*, 375−381.

(24) Li-Jung, Y.; Chen, M.-L.; Tzeng, S.-S.; Chiou, T.-K.; Jiang, S.-T. Properties of extracellular ice-nucleating substances from *Pseudomonas fluorescens* MACK-4 and its effect on the freezing of some food materials. *Fish. Sci.* **2005**, *71*, 941−947.

(25) Van Sleeuwen, R. M. T.; Lee, T. C. Influence of biogenic ice nucleators on characteristics of model food freezing: design of a predictive computer model. Ph.D. Dissertation, Rutgers, State University of New Jersey, New Brunswick, 2003.
(26) Watanabe, M.; Arai, S. Freezing of water in the presence of the ice nucleation active bacterium, *Erwinia ananas*, and its application for efficient freeze-drying of foods. *Agric. Biol. Chem.* **1986**, *51*, 557−563.
(27) Zasypkin, D. V.; Lee, T. C. Extracellular ice nucleators from *Pantoea ananas*: effects on freezing of model foods. *J. Food Sci.* **1999**, *64*, 473−478.
(28) Li, J.; Lee, T. C. Enhanced production of extracellular ice nucleators from *Erwinia herbicola*. *J. Gen. Appl. Microbiol.* **1998**, *44*, 405−413.
(29) Sean, X.; Liu, J.-T. K. Application of Kevin—Voigt model in quantifying whey protein adsorption on polyethersulfone using QCM-D. *J. Lab. Autom.* **2009**, *14*, 213−220.
(30) Zander, N.; Pappas, D.; Stein, B. *Oxidation of Polyethylene: A Comparison of Plasma and Ultraviolet Ozone Processing Techniques*; Army Research Laboratory: Adelphi, MD, 2009.
(31) Mathieson, I.; Bradley, R. H. Surface oxidation of poly ether ether ketone films using ultraviolet/ozone. *J. Mater. Chem.* **1994**, *4*, 1157.
(32) MacManus, L. F.; Walzak, M. J.; McIntyre, N. S. Study of ultraviolet light and ozone surface modification of polypropylene. *J. Polym. Sci., Part A: Polym. Chem.* **1999**, *37*, 2489−2501.
(33) Muryoi, N.; Matsukawa, K.; Yamade, K.; Kawahara, H.; Obata, H. Purification and properties of an ice-nucleating protein from an ice-nucleating bacterium, *Pantoea ananatis* KUIN-3. *J. Biosci. Bioeng.* **2003**, *95*, 157.
(34) Govindarajan, A. G.; Lindow, S. E. Size of bacterial ice nucleation sites measured in situ by radiation inactivation analysis. *Proc. Natl. Acad. Sci. U.S.A* **1988**, *85*, 1334−1338.
(35) Caram-Lelham, N.; Sundelöf, L.-O. Some aspects on characterization and properties of charged polysaccharides. An investigation of the system carrageenan/amitriptyline/water with relation to amphiphile adsorption and charge density. *Int. J. Pharm.* **1995**, *115*, 103.
(36) Isaksson, K.; Åkerberg, D.; Said, K.; Tingstedt, B. Cationic polypeptides in a concept of oppositely charged polypeptides as prevention of postsurgical intraabdominal adhesions. *J. Biomed. Sci. Eng.* **2011**, *4*, 200−206.